

AD_____

AWARD NUMBER: W81XWH-07-1-0583

TITLE: Immune Response Augmentation in Metastasized Breast Cancer by Localized Therapy Utilizing Biocompatible Magnetic Fluids

PRINCIPAL INVESTIGATOR: Cahit A. Evrensel, Ph.D.

CONTRACTING ORGANIZATION: University of Nevada, Reno
Reno, NV 89557

REPORT DATE: August 2009

TYPE OF REPORT: Final Addendum

PREPARED FOR: U.S. Army Medical Research and Materiel Command
Fort Detrick, Maryland 21702-5012

DISTRIBUTION STATEMENT: Approved for Public Release;
Distribution Unlimited

The views, opinions and/or findings contained in this report are those of the author(s) and should not be construed as an official Department of the Army position, policy or decision unless so designated by other documentation.

REPORT DOCUMENTATION PAGE			<i>Form Approved</i> <i>OMB No. 0704-0188</i>		
Public reporting burden for this collection of information is estimated to average 1 hour per response, including the time for reviewing instructions, searching existing data sources, gathering and maintaining the data needed, and completing and reviewing this collection of information. Send comments regarding this burden estimate or any other aspect of this collection of information, including suggestions for reducing this burden to Department of Defense, Washington Headquarters Services, Directorate for Information Operations and Reports (0704-0188), 1215 Jefferson Davis Highway, Suite 1204, Arlington, VA 22202-4302. Respondents should be aware that notwithstanding any other provision of law, no person shall be subject to any penalty for failing to comply with a collection of information if it does not display a currently valid OMB control number. PLEASE DO NOT RETURN YOUR FORM TO THE ABOVE ADDRESS.					
1. REPORT DATE 1 August 2009		2. REPORT TYPE Final Addendum		3. DATES COVERED 1 Aug 2008 – 31 Jul 2009	
4. TITLE AND SUBTITLE Immune Response Augmentation in Metastasized Breast Cancer by Localized Therapy Utilizing Biocompatible Magnetic Fluids			5a. CONTRACT NUMBER		
			5b. GRANT NUMBER W81XWH-07-1-0583		
			5c. PROGRAM ELEMENT NUMBER		
6. AUTHOR(S) Cahit A. Evrensel, Ph.D. (PI); Lisbeth Welniak, Ph.D. (Co-PI); Alan Fuchs, Ph.D. (Co-PI); Faramarz Gordaninejad, Ph.D. (Co-PI) E-Mail: cahit@unr.edu			5d. PROJECT NUMBER		
			5e. TASK NUMBER		
			5f. WORK UNIT NUMBER		
7. PERFORMING ORGANIZATION NAME(S) AND ADDRESS(ES) University of Nevada, Reno Reno, NV 89557			8. PERFORMING ORGANIZATION REPORT NUMBER		
9. SPONSORING / MONITORING AGENCY NAME(S) AND ADDRESS(ES) U.S. Army Medical Research and Materiel Command Fort Detrick, Maryland 21702-5012			10. SPONSOR/MONITOR'S ACRONYM(S)		
			11. SPONSOR/MONITOR'S REPORT NUMBER(S)		
12. DISTRIBUTION / AVAILABILITY STATEMENT Approved for Public Release; Distribution Unlimited					
13. SUPPLEMENTARY NOTES					
14. ABSTRACT During the second year Magneto-rheological Fluid (MRF) iron nano-particles were synthesized using the reverse micelle technique and coated with poly(NIPAAm). The size distribution of the nano iron particles was characterized using dynamic light scattering (DLS). The particle size was 730nm, and the Tg of the coating was characterized using DSC. The 80 wt.% MRF based on phosphate buffered saline (PBS) and iron particles was characterized using the shear rheometer in the range of shear rates from 1Hz – 400Hz at room temperature. Shear stress and shear viscosity of MRF was found to increase with the applied magnetic flux density. According to the Bingham model, the yield stress of MRF can be found by extrapolating the shear stress curve at zero shear rate. The mathematical model developed during the first year was used to explore the dynamics behavior of iron particles injected into tumor and resulting force and stress applied on the neighboring tissue under magnetic field. The effect of particle size on these values is investigated. Results showed that stress on the neighboring tissue is increased linearly with the increasing particle size.					
15. SUBJECT TERMS Cancer therapy by localized immune response, Magneto-rehological Fluids					
16. SECURITY CLASSIFICATION OF:			17. LIMITATION OF ABSTRACT UU	18. NUMBER OF PAGES 22	19a. NAME OF RESPONSIBLE PERSON USAMRMC
a. REPORT U	b. ABSTRACT U	c. THIS PAGE U			19b. TELEPHONE NUMBER (include area code)

Table of Contents

	<u>Page</u>
Introduction.....	1
Body.....	1
Key Research Accomplishments.....	8
Reportable Outcomes.....	8
Conclusion.....	9
References.....	9
Appendices.....	12

INTRODUCTION

The main goal of this research is to assess the efficacy of augmenting immune responses to breast cancer through the use of magneto-rheological fluid (MRF), suspensions of micron size ferrous particles in a carrier medium. It is hypothesized that tumor may be damaged, even killed, by injecting a biocompatible MRF into the tumor and by applying an external magnetic field resulting in temporary semi-solid aggregate formation within the tumor. This may initiate of “danger” signals (i.e. pro-inflammatory cytokine production) resulting from the locally high stress on the neighboring tissue due to attraction forces between the ferrous particles caused by the magnetic field applied and tumor disruption. The specific aims of the study are to: 1) Design and characterize biocompatible MRF with coated particles; 2) Develop computational model to explore the behavior of iron particles injected into tumor under magnetic field and maximize their response while minimizing the particle size, concentration to improve biocompatibility and biodegradability 3) Evaluate the effect of MRFs on tumors injected with MRF and immune responses to the tumor using animal models.

Main results were reported in the previous annual report submitted. This report includes additional results during the approved no cost extension period. During this second year the emphasis was on surface polymerization to the micron size particle, synthesis of nanoparticles and characterization of these materials. Also, the force and stress exerted on the neighboring tissue by iron particles were investigated computationally and the effect of particle size on them was explored.

BODY

Background

Traditionally, means to induce breast tumor regression has involved the use of surgery alone or with cytotoxic agents. However, chemotherapy and radiation therapy can kill off the immune effector cells as well as the tumor. Surgery results in removal of tumor burden such that the antigen pool is lost. Thus an alternate means therapy is needed if we wish to harness the potential of the immune system to help eliminate metastatic breast cancer. Injection of MRF into a primary tumor, followed by application of a magnetic field to the site may act augment immune responses to breast cancer through the induction of tumor death due to mechanical disruption of the tumor architecture. This will allow for antigen uptake, generation of “danger” signals allowing for augmentation of immune responses. Ultimately, this will allow for immune responses to disseminated disease. This combination of engineering, nanotechnology and immune attack represents a novel means to attack the cancer which could be applied to primary tumors such that disease eradication is possible.

Many types of controlled radical polymerization have been studied for surface polymerization of an inorganic substrate, such as atom transfer radical polymerization (ATRP), and reversible addition fragmentation chain transfer (RAFT). The resulting polymer has controlled topologies, narrow polydispersity index (PDI~1), various functionalities, block copolymers, and controlled composition [1, 2]. Various monomers can be polymerized using ATRP either at mild conditions or elevated temperature [1-3]. ATRP involves reversible redox reaction of organic halide initiator and metal halides, e.g.: cuprous halide, as a catalyst, and a ligand to improve the solubility of the metal salt in the organic reaction system [2]. The application of ATRP for

surface polymerization of iron particles has been investigated by Fuchs et. al. [4]. The iron particles have been coated using poly(butyl acrylate) and poly(fluorostyrene). Surface modified iron particles were used in magnetorheological fluid (MRF) and magnetorheological elastomer (MRE) applications [1]. The grafting technique for thermally responsive poly(*N*-isopropylacrylamide) poly(NIPAAm) onto silica nanoparticles using ATRP has been investigated by [5, 6]. In the present work, MRFs were synthesized from suspensions of iron particles in carrier fluids, which contain phosphate buffered saline (PBS). The iron particles have been surface coated using atom transfer radical polymerization (ATRP) with various polymers, such as poly(*N*-isopropylacrylamide) (poly(NIPAAm)), poly(acrylamides) (poly(AAm)) and poly(NIPAAm-co-AAm). Thermal transition temperature of surface grafted polymers was characterized using differential scanning calorimetry (DSC). Nanosize iron particles were synthesized using the reverse micelle technique. The rheological properties of MRF were characterized using a shear rheometer. In addition, the simulant material for breast cancer was synthesized using silicone gel.

Breast cancer tumor is a viscoelastic material with about 3kPa shear modulus [7]. Understanding the dynamics of particles under magnetic field is essential to predict their behavior after injection of MRF into a tumor and to choose the proper particle size and concentration. Controllable magnetic force attracts the particles toward the region of highest field gradient which are the poles of the magnet [8, 9]. Force-displacement relationship for a spherical particle in an elastic media was developed by Lin et. al. [10]. These forces, together with other forces such as particle-particle interaction have been used to model dynamic behavior of particles injected into a tumor under a magnetic field and the resulting stress on the neighboring tissue. A similar model was developed to study particle and flow dynamics in 2-dimensional micro channels previously by our group [11].

With the advances in recent medicine, biocompatible magnetic particles are beginning to play a major role in advancing and improving various methods of medical treatment. Since drugs with effective results during in vitro trials often spend more time under in vivo trials due to the inefficiency of an effective drug delivery, significant amount of research is concentrated on perfecting the targeted drug delivery approach. Hence, Forbes et al presented both experimental and theoretical models which used magnetic micro particles for a site-specific drug delivery [12]. They proposed a method for a site-specific drug delivery by applying a uniform magnetic field to an injected superparamagnetic colloidal fluid carrying a specified drug. Their results showed that it is indeed possible to capture magnetic particles at specified locations, and also that a Non-Newtonian blood flow will cause the particles to create random migrations by diffusion. Hence, these magnetic particles could also be used to block microvessels not accessible by catheter, as a mean of starving the tumors. Another heavily proposed use of these particles has been to artificially induce hyperthermia. A clear advantage of this treatment is to ensure that only the targeted tissue is heated as opposed to a healthy tissue. The principal investigation dates back to 1957 when Gilchrist et al heated various tissue samples with 20–100 nm size particles of γ - Fe₂O₃ exposed to a 1.2MHz magnetic field [13, 14]. Since then many have investigated this treatment using an AC magnetic field to vibrate the magnetic particles to damage the targeted tissue [15]. Depending on the strength of the field and the frequency of the particles, this in turn

heats up the particles. As discussed by Pankhurst et al, heating the surrounding tissue to a threshold of 42°C for 30 min or more, the cancer will be destroyed [14].

Hypothesis and Specific Aims

It is hypothesized that the injection of MRF intra-tumorally followed by magnetic treatment will result in necrotic tumor death by mechanical injury, release of tumor antigen and activation of localized inflammatory response. This hypothesis is tested by the following specific aims:

- 1- MRF Synthesis: Design and develop MRF with desired rheology for the proposed study.
 - Iron particle surface coating by atom transfer radical polymerization (ATRP) with various polymers.
 - Characterization of surface coating and MRF using differential scanning calorimetry, and rheometer
- 2- Mathematical model: Develop a computational model to simulate the behavior of iron particles injected into tumor under magnetic field
 - Motion of particles inside the elastic media.
 - Stress applied by the particles on the elastic media (tumor)
- 3- Orthotopic 4T1 Mammary Cancer Model: Determine the effects of MRF and magnet treatment on:
 - Immediate and late histological changes (i.e. necrosis, edema, cellular infiltration).
 - Induction of apoptotic and stress responses in the primary tumor.
 - Innate and adaptive immunological responses to the tumor
 - Distant and metastatic tumors

Results

MRF Synthesis Characterization

Surface polymerization

Micron-size iron particles were bought from BASF and were imaged using scanning electron microscopy (SEM). The SEM image of micron-size iron particles is shown in Figure 1. Iron particles were washed with distilled water and ethanol respectively. ATRP is used to attach a polymer at the surface of the iron particles. Then, they were dried in a vacuum oven at 50 °C and under nitrogen purge for 24 hours and cooled down. Dried iron particles were reacted at 85 °C with CTCS for 24 hours under nitrogen with toluene as a solvent. The mixture was then filtered and washed with methanol in order to remove excess CTCS. The residue (Fe-CTCS) was dried in a vacuum oven at ~40-50°C for 24 hours. Then, functionalized Fe-CTCS was reacted with CuBr, CuBr₂, Spartein, and monomer in organic solvent at 85 °C for 24 hours under nitrogen. Finally, the mixture was filtered, washed several times with ethanol and dried in a vacuum oven at ~40-50°C prior to use [1]. The ATRP mechanism for surface polymerization is shown in Figure 2.

Differential scanning calorimetry (DSC) has been used to analyze the presence of polymer on the surface of iron particles and the thermal transition temperature of the grafted polymers. The individual thermal transition temperature, signified by large change of heat supplied (heat flow endo up – Y-axis). Then, the thermal transition temperatures from experiments were compared with available data from the literature. Literature values have been found for non-grafted polymers. On the other hand, the glass transition temperature of polymer grafted onto the surface of iron particles was measured in the experiments. Differences in glass transition temperatures between literature and experiment were probably caused by the decreased mobility of the polymer due to the covalent bonding on the surface of the iron particles. The results were in agreement with literature [16] which compared the thermal transition temperature between polystyrene and grafted polystyrene onto the surface of silica oxide. The literature value was approximately 20 °C higher for the grafted polymer. The glass transition temperature of a variety of polymers is shown in Table 1 and the DSC results for several polymers are shown in Figure 3.

Synthesis of iron nano-particles using the reverse micelle technique.

Iron nano-particles were synthesized using procedures described in [17]. Micelles were formed by adding Na – AOT to water and cyclohexane as the continuous phase. Two different samples of reactants were prepared. The first sample contains $\text{FeSO}_4 \cdot 7\text{H}_2\text{O}$ + Na – AOT + water + cyclohexane, and second sample contains NaBH_4 + Na – AOT + water + cyclohexane. Then, the reactants were mixed under nitrogen to avoid oxidation at room temperature. Finally, the product was washed using ethanol to remove the impurities. The size distribution of synthesized nano iron particles was characterized using DLS with ethanol as a liquid media and it is shown in Figure 4. In addition, the nano-size iron particles were also coated with poly(NIPAAm) and the polymer thermal transition was characterized using DSC. The resulting thermal transition was close to poly(NIPAAm) which was coated on the micron size iron particle. GE Ferridex and nano-size iron particles, which were synthesized in our lab were not characterized further because the magnetic permeability of nano-size iron particles is low compared with micron size iron particles [18]. In addition, after review of the magnetic particles available, the GE Ferridex was not selected because it does not have the functional species present on the surface, that are necessary for reaction of covalently bonded species. Also, these particles are available in very small size, 80-150 nm which are too small to provide substantial magnetic forces on the system. Also, it is coated with Dextran, which does not provide reactive sites for covalent interactions. Furthermore, the magnetic particles that were commercially available (Invitrogen and others) have other reactive species which allowed the multifunctional species to be reacted.

The 80 wt.% MRF based on phosphate buffered saline (PBS) and iron particles was characterized using the shear rheometer in the range of shear rates from 1Hz – 400Hz at room temperature. Shear stress and shear viscosity of MRF was found to increase with the applied magnetic flux density. According to the Bingham model, the yield stress of MRF can be found by extrapolating the shear stress curve at zero shear rate. For instance, the dynamic yield stress at 0.528 Tesla, the shear stress and shear viscosity of MRF was about 1.2×10^4 Pa and 30 Pa.s. Rheological properties of this type of MRF have high uncertainty values because the iron particles have a dispersion problem in the low viscosity PBS solution. The reported shear stress of MRF based on N-Octyl pyrrolidone was about 3.0×10^4 Pa [4]. Shear stress and shear viscosity

behavior of MRF as a function of shear rate for different magnetic flux density is shown in Figure 5 and Figure 6, respectively.

Mathematical Model

Behavior of the spherical iron particles injected into the breast cancer tumor under magnetic field is studied. For modeling purposes, only three particles are simulated inside an elastic media 3cm by 3cm in size. These three particles were then subjected to a non-uniform magnetic field, which was opposed by the force generated by the elastic medium. Particles were considered to be stationary when the magnetic field is turned on. Although the tumor is modeled as an elastic media a damping force is added to reduce the simulation time. This “arbitrary” force can be justified by considering that the goal is to predict the force when the particles settle at their new equilibrium position under magnetic field. Schematic of forces action on a particle are shown in Figure 7.

The force-displacement relationship for particles inside a homogenous, isotropic, linear incompressible elastic medium is given by Lin et. al. [10]:

$$F_{elastic} = 6\pi\delta R_0 G$$

Where G is shear modulus of the elastic media, δ is the distance travelled by the particle and R_0 is the radius of the spherical particle. Shear modulus of a Breast Cancer tumor is reported as 2900 Pa [7]. This force will act in both x and y direction, thus opposing the attraction of the particles towards the magnet.

The total magnetic force felt by each particle can be described as [19, 20]:

$$\vec{F} = (\vec{\nabla} \cdot \vec{m})\vec{H}_o = \vec{\nabla}(\vec{m} \cdot \vec{H}_o) - \vec{H}_o \cdot \nabla \vec{m} - \vec{m} \times (\vec{\nabla} \times \vec{H}_o) - \vec{H}_o \times (\vec{\nabla} \times \vec{m})$$

where \vec{H}_o is the applied field given by:

$$H_o = \frac{B}{\mu}$$

Here B is the induction field of the magnet, is assumed to be 0.2 T in this portion of the study, and μ_o is the space permeability, approximated to $4\pi \times 10^{-7}$. Since the dipole moment, \vec{m} , for each particle is assumed to be a constant, and since there is zero electric current flow, (ie $\vec{\nabla} \times \vec{H}_o = 0$), the expression can be further simplified as:

$$\vec{F} = (\vec{\nabla} \cdot \vec{m})\vec{H}_o = \vec{\nabla}(\vec{m} \cdot \vec{H}_o)$$

Since the magnetic field is not assumed to be uniform, there will a force on each particle, i , due to this external gradient. This gradient can be represented as:

$$\begin{aligned}\vec{F}_{i,x}^{gradient} &= \vec{m}_{i,x} \left(\frac{\partial \vec{H}_{i,x}}{\partial x} \right) + \vec{m}_{i,y} \left(\frac{\partial \vec{H}_{i,y}}{\partial x} \right) \\ \vec{F}_{i,y}^{gradient} &= \vec{m}_{i,x} \left(\frac{\partial \vec{H}_{i,x}}{\partial y} \right) + \vec{m}_{i,y} \left(\frac{\partial \vec{H}_{i,y}}{\partial y} \right)\end{aligned}$$

In order to calculate the dipole moment, \vec{m} , the following equation was used [20]:

$$\vec{m} = \vec{M} \mu_o V$$

where \mathbf{M} represents the Magnetization, V is the volume of each particle, and μ_o is the permeability of the fluid. Magnetization in both directions is calculated using the following equations:

$$\begin{aligned}\vec{M}_{i,x} &= 3 \left(\frac{\chi}{\chi + 3} \right) \vec{H}_{i,x} \\ \vec{M}_{i,y} &= 3 \left(\frac{\chi}{\chi + 3} \right) \vec{H}_{i,y}\end{aligned}$$

where χ represents the magnetic susceptibility of the particle, and H is the field generated by the permanent magnet.

The magnetic field vector can be represented as:

$$\mathbf{H} = -\nabla \varphi_m$$

where (φ_m) is the magnetic scalar potential. Due to the magnetic moment, it produces an elementary magnetic scalar potential given by:

$$d\varphi_m = \frac{1}{4\pi} \frac{\mathbf{R} d\mathbf{m}}{R^3} = \frac{1}{4\pi} \frac{\mathbf{R} \mathbf{M}}{R^3} dV'$$

where $\mathbf{R} = |\mathbf{r} - \mathbf{r}'|$ is the distance from the point where the magnetic field is being calculated to the elementary source, and $\mathbf{R} = \mathbf{r} - \mathbf{r}'$. However, due to the high velocity of the particles as they near the magnet, a simplified linear expression for the magnetic field was used when the particles were close to one micrometer away from the magnet. This method was justified because the particle is so close to the top of the magnet that a linear expression prevented the problem from diverging, and the magnitude of force experienced with the linear expression was accurate to

within ten percent error in the magnitude when compared with force calculated from the real magnetic field.

Under the effect of the magnetic field, the colloidal forces are dominated by the polarization forces acting on each particle [21]. In order to prevent the particles from entering each other, a short range repulsive force was implemented.

$$\vec{F}_i^{rep} = \sum_{j=1}^n \frac{|\vec{m}_i| |\vec{m}_j|}{4\pi\mu_o (2a_p)^4} e^{\left[-40\left(\frac{|\vec{r}_{ij}|}{a_p} - 1\right)\right]}$$

This exponential repulsive provides a greater force as the distance between two dipoles is reduced, and as the distance increases, the force slowly decays to zero.

For this simulation, the force generated by two magnetized dipoles was ignored along with the gravitational force. Since the medium is approximately three centimeters, the dipole-dipole interaction force was negligible as the elastic and the magnetic forces were the dominant forces acting on each particle. The repulsive force was negligible when compared with the elastic and magnetic force; however, it was required in order to prevent the particles from going through each other.

Finally, two damping forces are imposed on each particle. The first damping force acts when the particles are moving about the medium, and the second damping force acts only when the particles get close to the tumor boundary and prevents the particles from going beyond those dimensions. The constants for these damping forces are chosen to reduce the simulation time. Somewhat arbitrariness of these numbers can be justified by considering that the main goal of the simulation is to determine final location of the particle and the resulting force on the neighboring tissue.

$$F_{wall} = -b\dot{x}$$

$$F_{damping} = -c\dot{x}$$

Here b was approximated to be 0.00006 N-s/m, and c was approximated to be $5 \cdot 10^{-8}$ N-s/m. The damping force and the wall force acted in both the x-y direction.

First set of results are presented for three particles at different locations in the tumor (Figure 8). Particles are assumed to be at rest when the magnetic field is applied. Resulting displacement, elastic force on the particle (force on the tissue by the particle) and average stress on the tissue in contact with the particle are given on Tables 2 and 3.

Figure 9 shows the response for y direction of particle B from Table 3 inside the elastic medium. The motion damps out due to damping included.

One of the goals of this analysis is to evaluate the effect of the particle size on the force and stress applied on the neighboring tissue. For this purpose five different particle sizes are chosen, ranging from 0.5 micron to 8 micron Table 4 show the effects of varying the size for particles A, B, and C on the resulting force and stress applied on the tissue, respectively. They are assumed to be centered about the magnet to reduce the simulation time.

Variation of the force applied on the neighboring tissue by the particle A for the same magnetic field and location is shown in Figure 10. The force increases drastically with increasing particle size. Figure 11 graphically shows the relationship between resultant stress and an increasing particle size. These results indicate that force and resulting stress on the tissue increases with increasing particle size. This relationship for the stress is linear as it should be expected. Since the applied force by the magnetic field is proportional to volume of the particle (3^{rd} power of the radius) while area is proportional to the 2^{nd} power of the radius, their ratio, stress, is expected to be linear function of the particle radius.

KEY RESEARCH ACCOMPLISHMENTS

- Different polymers were grafted onto the surface of iron particles. The glass transition temperature of these grafted polymers were higher than bulk polymer which is most likely caused by decreased mobility of the polymer due to covalent bonding of the polymer to the surface of the iron particles.
- The computational model developed to investigate the dynamic behavior of MRF injected into a tumor with the external magnetic field application during the previous reporting period is used to investigate forces and stresses applied on the neighboring tissue and to explore the effect of the particle size on them.

REPORTABLE OUTCOMES

The following papers were presented and published in the conference proceedings during the second year

Myriam N. Bouchlaka, Alan Fuchs, Cahit A. Evrensel, Lisbeth A. Welniak and William J. Murphy, Mechanical disruption of the primary tumor using biocompatible magnetic beads in combination with immunotherapy allows for systemic anti-tumor responses in metastatic breast cancer, International Society for Biological Therapy of Cancer (iSBTc) 23rd Annual meeting, San Diego, October 31 - November 2, 2008

Evrensel, C.A., Welniak, L., Fuchs, A., Patel, J., Murphy W.J., Gordaninejad F., Utilization of Biocompatible Ferrous Particles for a New Cancer Therapy, *ASME Summer Bioengineering Conference*, 2009

CONCLUSION

Iron nano-particles were synthesized using the reverse micelle technique and coated with poly(NIPAAm). Shear stress and shear viscosity of MRF were found to increase with the applied magnetic flux density. According to the Bingham model, the yield stress of MRF can be found by extrapolating the shear stress curve at zero shear rate.

A computational model was developed to investigate the dynamic behavior of particles injected into an elastic media with properties of a breast tumor. This model is used to investigate effect of the particle size on the force and stress applied on the neighboring tissue change. The results indicate that stress increases with the particle size linearly.

REFERENCES

1. J. Sutrisno, "Surface Polymerization of Iron Particles for Magnetorheological Elastomers (MREs) and Their Potential Application as Sensors", Chemical Engineering Master Thesis, UNR, 2008
2. G. Odian, "Principles of Polymerization", John Willey and Sons, Inc., 2004
3. K. Matyjaszewski, and J. Xia, "Atom Transfer Radical Polymerization", Chem. Rev., Vol. 101, pp. 2921 – 2990, 2001.
4. B. Hu a, A. Fuchs, S. Huseyin, F. Gordaninejad, and C. Evrensel, "Atom transfer radical polymerized MR fluids", Polymer, Vol. 47, pp. 7653 – 7663, 2006.
5. T. Wu, Y. Zhang, X. Wang, and S. Liu, "Fabrication of Hybrid Silica Nanoparticles Densely Grafted with Thermoresponsive Poly(Nisopropylacrylamide) Brushes of Controlled Thickness via Surface-Initiated Atom Transfer Radical Polymerization", Chem. Mater., Vol. 20, pp. 101 – 109, 2008
6. K. Nagase, J. Kobayashi, A. Kikuchi, Y. Akiyama, H. Kanazawa, and T. Okano, "Effects of Graft Densities and Chain Lengths on Separation of Bioactive Compounds by Nanolayered Thermoresponsive Polymer Brush Surfaces", Langmuir, Vol. 24, pp. 511 – 517, 2008
7. R. Sinkus, M. Tanter, T. Xydeas, S. Catheline, J. Bercoff, and M. Fink, Viscoelastic Shear Properties of In Vivo Breast Lesions Measured by MR Elastography, Magnetic Resonance Imaging, vol. 23, pp. 159-165, 2005
8. Mohebi M., Jamasbi N., and Liu J., "Simulation of the Formation of Non-equilibrium structures in Magnetorheological Fluids Subject to an External Magnetic Field", *Physical Review E* **54**, No: 5, pp 5407, 1996

9. Wang Z., Holm C., and Muller H.W., “Molecular Dynamics Study on the Equilibrium Magnetization Properties and Structure of Ferrofluids”, *Physical Review E* **66**, 021405, 2002.
10. Lin, D.C.; Langrana, N.A.; Yurke, B., Force-displacement relationships for spherical inclusions in finite elastic media, *Journal of Applied Physics*, Vol.97, no.4, pp. 4351-14, 2005
11. Ozcan, S.; Evrensel, C.A.; Pinsky, M.A.; Fuchs, A., Dynamic Simulation Of Pressure Driven Flow Of Fluids With Suspended Ferrous Particles In A Micro Channel Under Magnetic Field, *International Journal of Modern Physics B*, Vol. 21 Issue 28/29, pp. 4890-4897, 2007
12. Forbes, Zachary, Yellen, Benjamin B., Barbee, Kenneth, and Friedman, Gary. “An Approach to Targeted Drug Delivery Based on Uniform Magnetic Fields.” IEEE Transactions on Magnetics 39-5 (2003): 3372-3377
13. Gilchrist R K, Medal R, Shorey W D, Hanselman R C, Parrott J C, and Taylor C B. “Selective inductive heating of lymph nodes” Ann. Surg. 146 (1957): 596–606
14. Pankhurst, Q A, Connolly, J, Jones, S K, and Dobson J. “Applications of magnetic nanoparticles in biomedicine.” Journal of Physics D: Applied Physics 36 (2003) R167–R181
15. Hilger, Ingrid, Hergt, Rudolf, and Kaiser, Werner. “Towards breast cancer treatment by magnetic heating.” Journal of Magnetism and Magnetic Materials 293 (2005): 314-319
16. H. Zhang, X. Lei, Z. Su, and P. Liu, “A novel method of surface-initiate atom transfer radical polymerization of styrene from silica nanoparticles for preparation of monodispersed core-shell hybrid nanospheres”, *J. Polym. Res.*, Vol. 14, pp. 253 – 260, 2007
17. O. A. Graeve, and K. Sinha, “Dynamic Light Scattering Study of Reverse Micellar System for the Synthesis of Iron-Based Nanofluids”, *International Journal of Modern Physics B*, Vol. 21, pp. 4774 – 4781, 2007
18. J. P. Jakubovics, “Magnetism and Magnetic Materials 2nd ed.”, London, Institute of Materials, 1994.
19. Mladenovic, Ana, and Aleksic, Slavoljub. “Determination of magnetic field for different shaped permanent magnets.” Electromagnetic Compatibility and Electromagnetic Ecology (2007): 84-87
20. Rosensweig, R.E. Ferrohydrodynamics. Mineol: Dover Publications, INC, 1985

21. Tomofumi Ukai and Toru Maekawa, "Patterns Formed by Paramagnetic Particles in a Horizontal Layer of a Magnetorheological Fluid Subjected to a DC Magnetic Field", *Physical Review E* 69, 032501, 2004
22. I. Jaginova, K. Csornorova, M. Stillhammerova, and J. Barton, "Differential Scanning Calorimetry and Thermogravimetry Studies of Polyacrylamide Prepared by Free-radical Polymerization in Inverse Microemulsion and in Solution", *Macromol. Chem. Phys.*, Vol. 195, pp. 3609 – 3614, 1994
23. R. G. Sousa, W. F. Magalhaes, and R. F. S. Freitas, "Glass Transition and Thermal Stability of Poly(N-Isopropylacrylamide) Gels and Some of Their Copolymers With Acrylamide", *Polymer degradation and stability*, pp. 275-281, vol. 61, 1998

APPENDIX: SUPPORTING DATA

Tables

Table 1 – Tg of grafted polymer and literature

Grafted polymers	Experiment (°C)	Literature (°C)
Poly(AAm)	218.7	196 [22]
Poly(NIPAAm-co-AAm)	156.2	143.5 (50:50 weight ratio) [23]
Poly(NIPAAm)	235	135 [23]

Table 2. Resultant Stress for a set of random locations.

	X - Location (m)	Y - Location (m)		Resultant Elastic Force (N)	Resultant Stress (Pa)
	Start	Start	End		
Particle A	1.00E-02	1.33E-08	2.64E-08	1.54E-09	1.22E+02
Particle B	1.00E-02	6.00E-06	6.01E-06	1.54E-09	1.23E+02
Particle C	1.50E-02	2.95E-02	2.95E-02	6.11E-09	4.86E+02

Table 3 Resultant Stress for a second set of locations.

	X - Location (m)	Y - Location (m)		Resultant Elastic Force (N)	Resultant Stress (Pa)
	Start	Start	End		
Particle A	1.00E-02	1.33E-08	2.64E-08	1.54E-09	1.22E+02
Particle B	0.00E+00	1.50E-02	1.50E-02	1.74E-08	1.38E+03
Particle C	0.00E+00	2.98E-02	3.00E-02	2.05E-05	1.63E+06

Table 4. Varying size for the particles.

Particle Radius	Location of A (y = 1.33E-08 m)		Location of B (y = 1.50E-02 m)		Location of C (y = 2.20E-02 m)	
	Force (N)	Stress (Pa)	Force (N)	Stress (Pa)	Force (N)	Stress (Pa)
5.00E-07	2.27E-10	7.21E+01	1.81E-09	5.77E+02	1.20E-08	3.80E+03
1.00E-06	1.81E-09	1.44E+02	1.45E-08	1.15E+03	9.57E-08	7.61E+03
2.00E-06	1.45E-08	2.89E+02	1.16E-07	2.31E+03	7.67E-07	1.53E+04
4.00E-06	1.16E-07	5.77E+02	9.29E-07	4.62E+03	6.18E-06	3.08E+04
8.00E-06	9.28E-07	1.15E+03	7.45E-06	9.26E+03	5.12E-05	6.36E+04

Figures

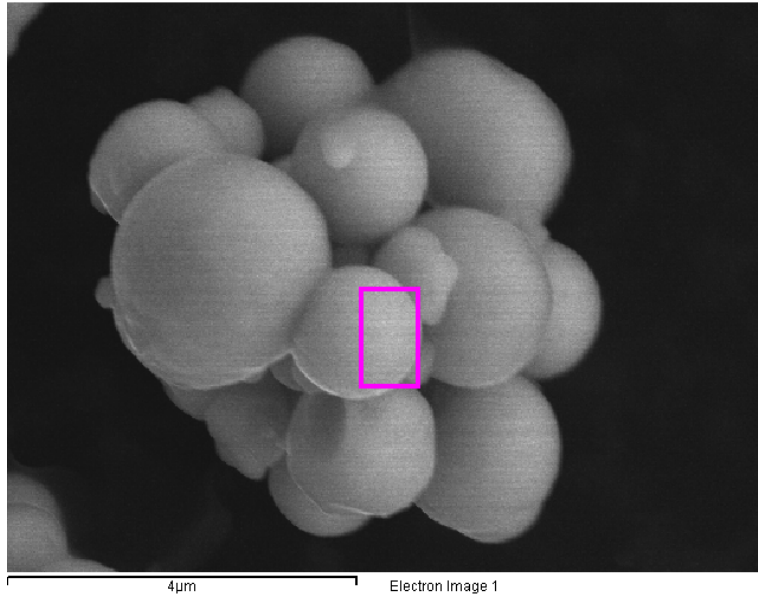


Figure 1 – SEM image of micron-size iron particles.

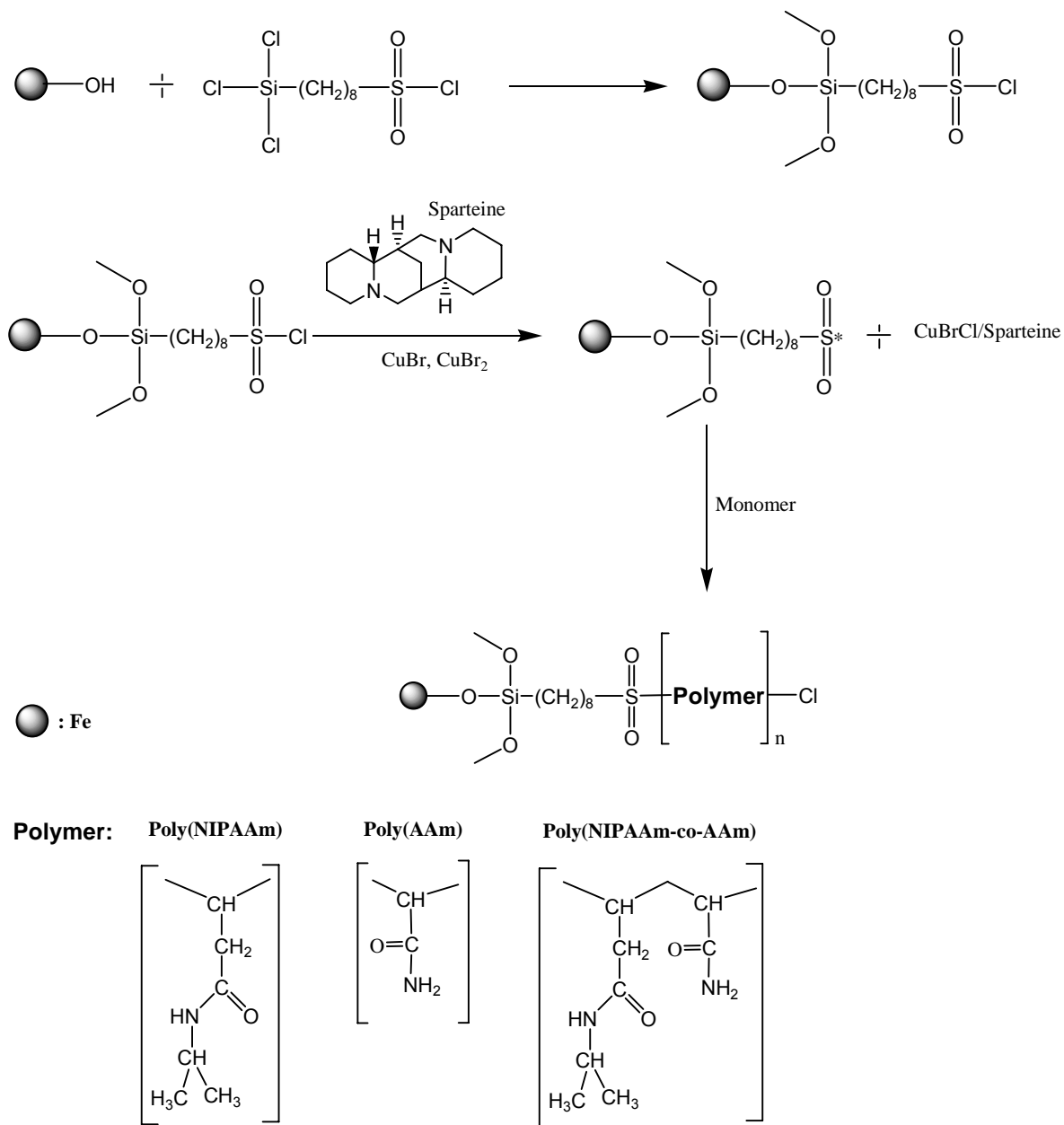


Figure 2 - Surface polymerization poly(NIPAAm) and poly(AAm) on the iron particles using ATRP.

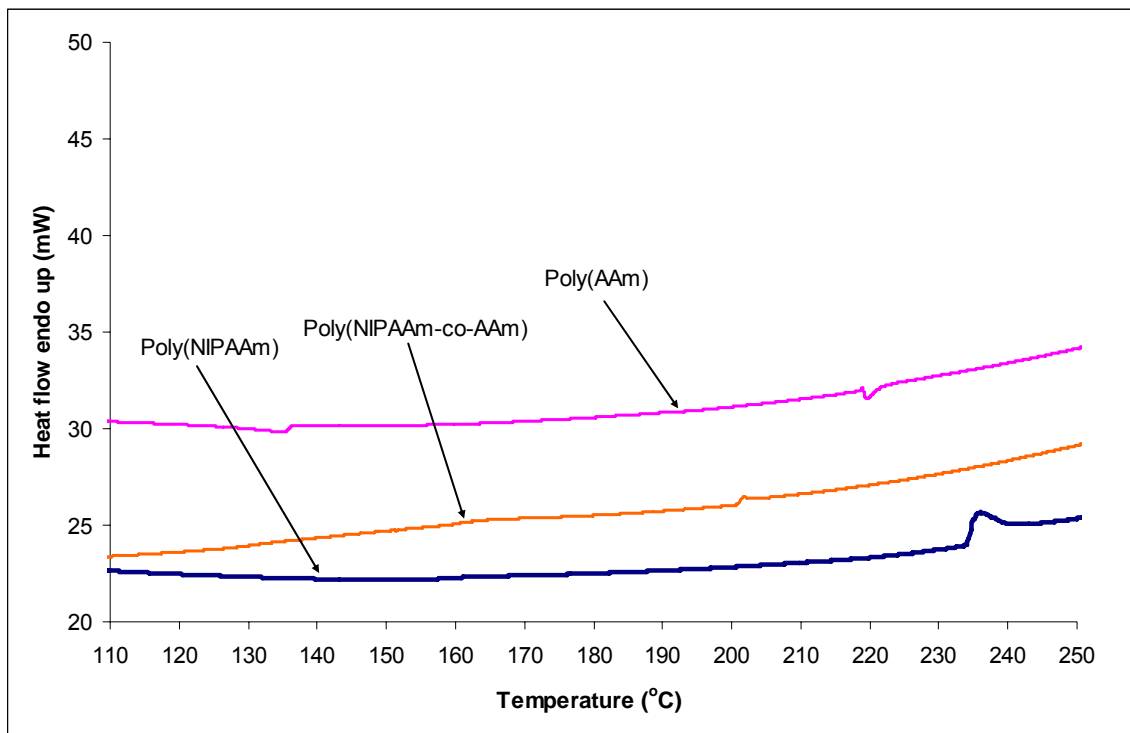


Figure 3 – DSC result of surface grafting of various polymers

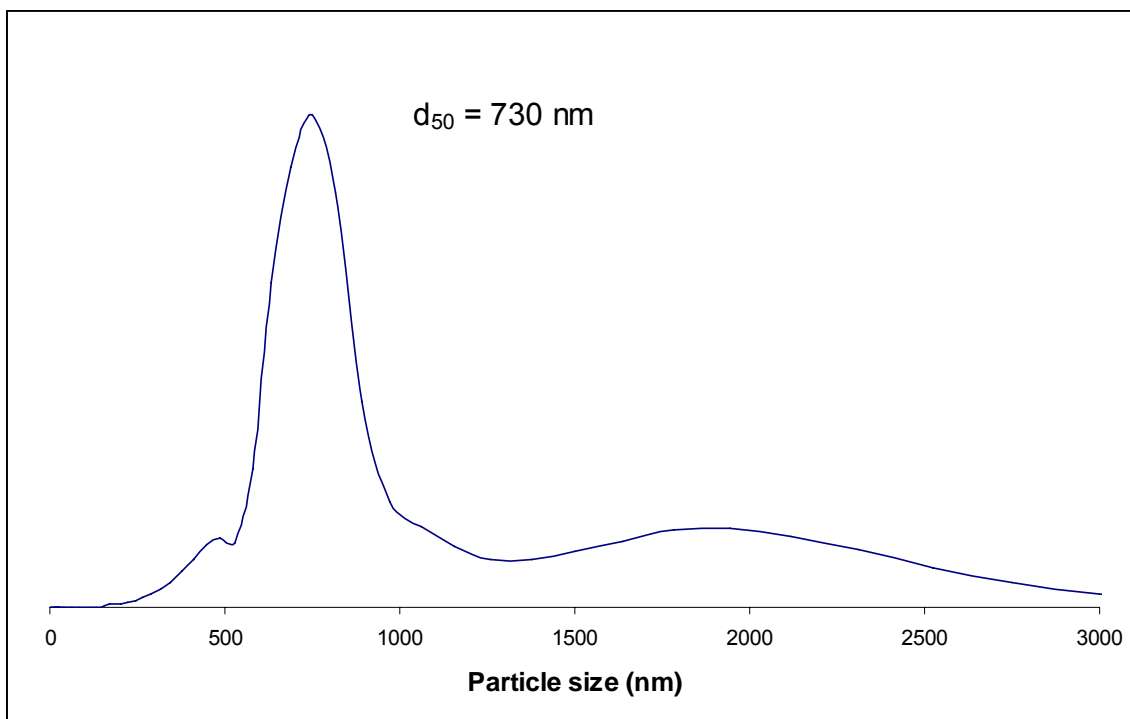


Figure 4 – DLS result of nano iron particles using reverse micelle technique with average particle size 730 nm.

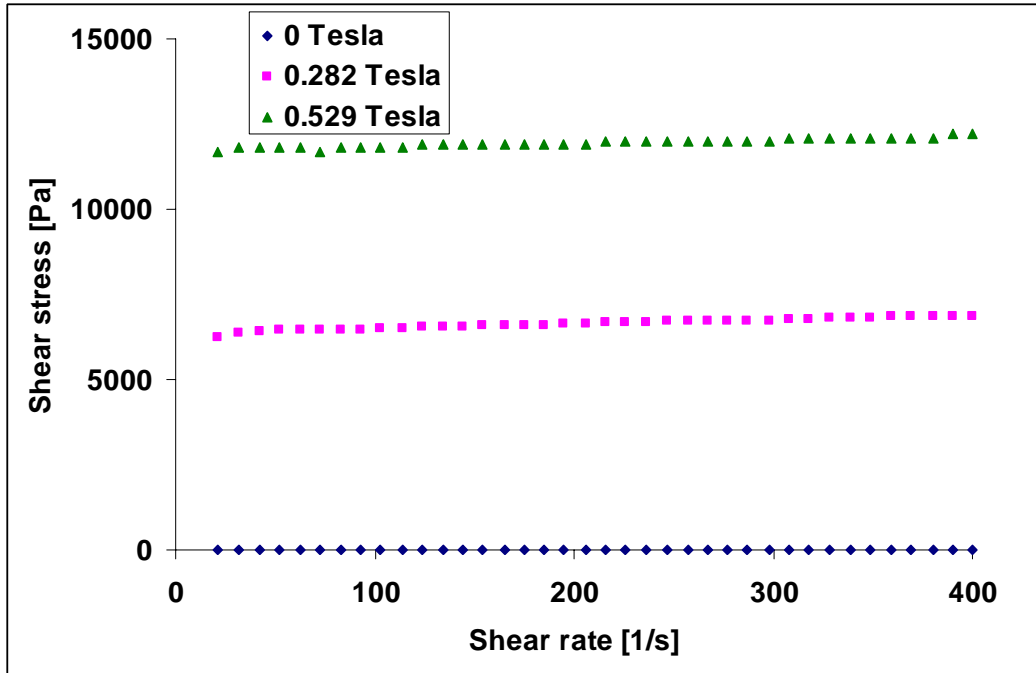


Figure 5 - Shear stress and shear viscosity behavior of 80 wt.% MRF as a function of shear rate for different magnetic flux density.

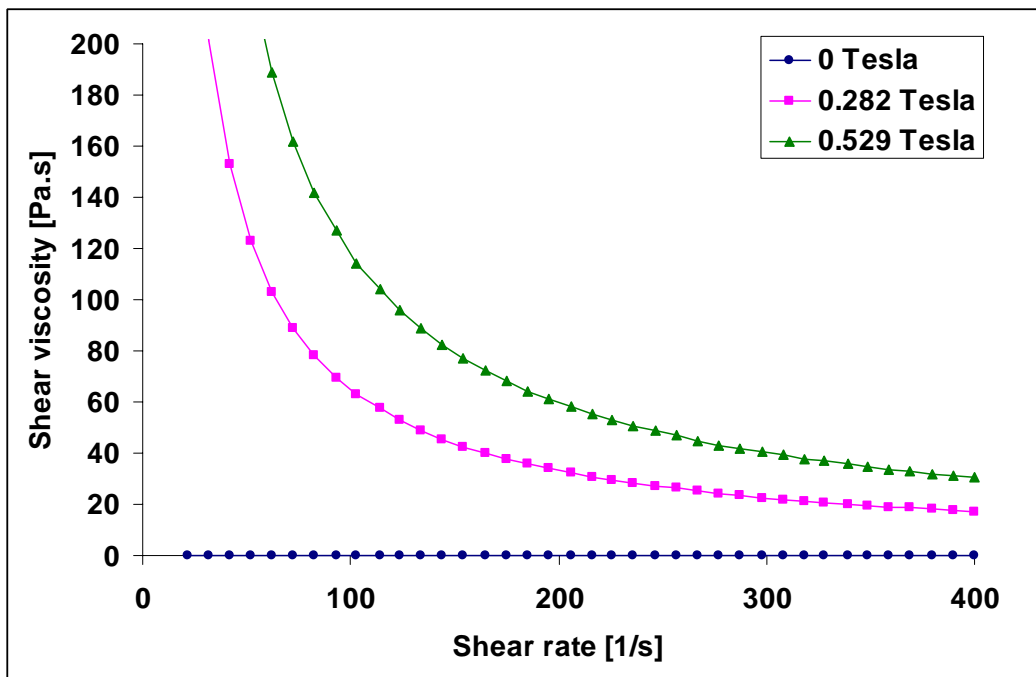


Figure 6 - Shear viscosity behavior of 80 wt.% MRF as a function of shear rate for different magnetic flux density.

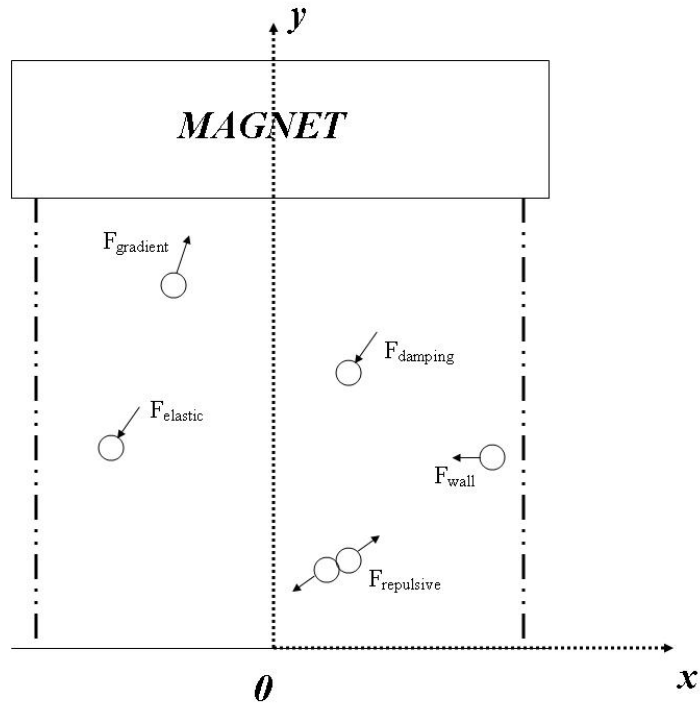


Figure 7. Orientation of the magnet, and forces acting on each particle.

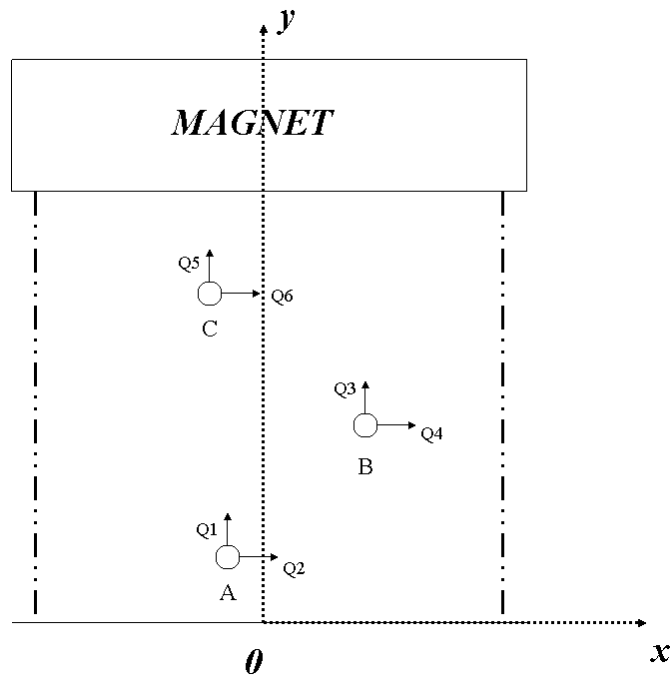


Figure 8. Locations/ directions for each particle.

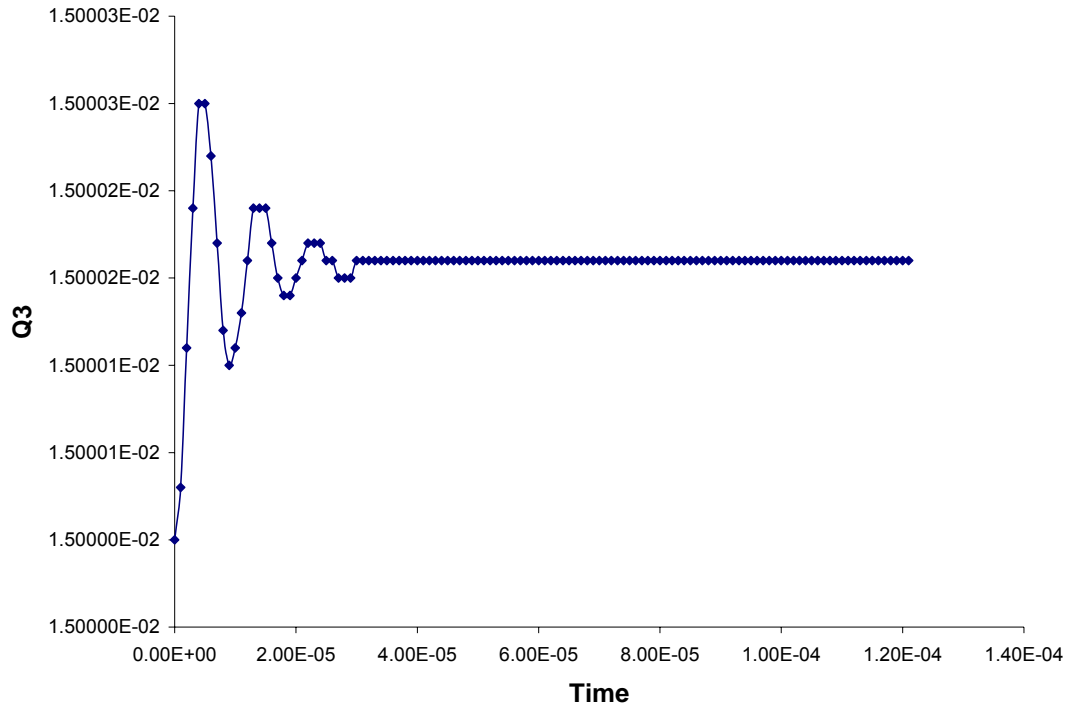


Figure 9. Q3 vs. Time.

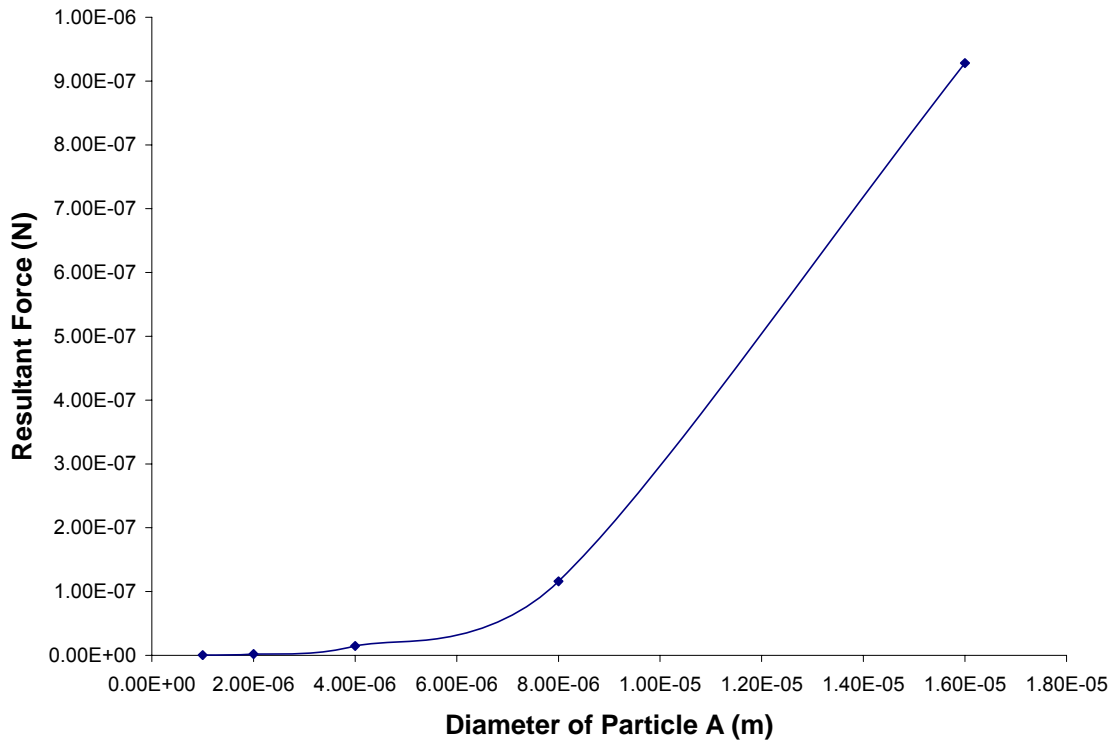


Figure 10. Force vs. diameter for particle A.

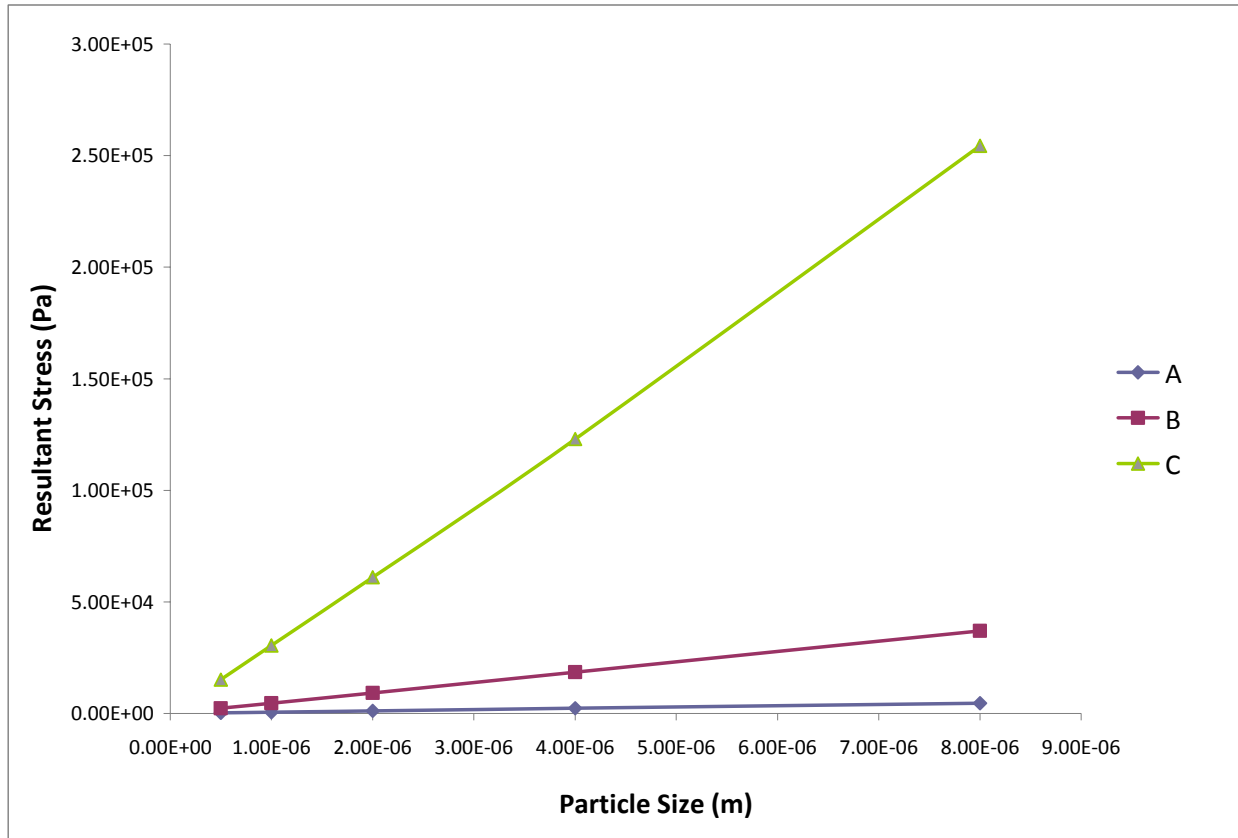


Figure 11 Resultant Stress versus Particle size.